Krisandi-(3)_Assessing saturated hydraulic conductivity from the dielectrically-predicted dry bulk density

by Krisandi Wijaya

Submission date: 02-Apr-2023 09:21PM (UTC+0700)
Submission ID: 2053458950
File name: ductivity_from_the_dielectrically-predicted_dry_bulk_density.pdf (532.77K)
Word count: 4519
Character count: 22874

Assessing saturated hydraulic conductivity from the dielectrically-predicted dry bulk density

Krissandi Wijaya[1*], Purwoko Hari Kuncoro[1], Taku Nishimura[2], Budi Indra Setiawan[3]

(1. Faculty of Agriculture, Jenderal Soedirman University, Jl. dr. Soeparno No. 61, Karangwangkal, Purwokerto 53123, Central Java, Indonesia;
2. Graduate School of Agricultural and Life Sciences, The University of Tokyo, Yayoi 1-1-1, Bunkyo-ku, Tokyo 113-8657, Japan;
3. Department of Civil and Environmental Engineering, Bogor Agricultural University, Kampus IPB Darmaga, Bogor 16680, West Java, Indonesia)

Abstract: Direct measurement of saturated hydraulic conductivity (K_s) and dry bulk density (ρ_b) is often laborious, time consuming, and expensive. Predicted dry bulk density ($\rho_{b\text{-}ADR}$) using amplitude domain reflectometry (ADR) probe has been employed to predict saturated hydraulic conductivity (K_{s_ADR}) after a slight modification on the previously available non-similar media concept (NSMC) model. All the predicted values were validated using the corresponding measured data of 108 undisturbed samples for each of 0-15 and 15-30 cm soil depths observed. The proposed "Dielectric NSMC" model could describe ρ_{b_ADR} dependencies of K_{s_ADR} better than the other proceeding models for both ranges of soil depths observed. The proposed model tended to slightly underestimate the measured saturated hydraulic conductivity (K_{s_meas}) as implied from the negative value of mean difference (MD). The scattering pattern of data which was well supported by the small value of root mean square error (RMSE) and relative root mean square error (rRMSE), however, suggested a small deviation of the K_{s_ADR} from the K_{s_meas}. Thus, the proposed model was considered sufficient for characterizing ρ_{b_ADR} dependencies of K_{s_ADR}. Effectiveness and practical merit of the ρ_{b_ADR} prediction rather than the conventional direct measurement of ρ_b, in particular, might promote a certain advantage for smoother fitting parameters.

Keywords: amplitude domain reflectometry (ADR) probe, dry bulk density, non-similar media concept (NSMC), pedo-transfer function, saturated hydraulic conductivity.

Citation: Wijaya, K., P. H. Kuncoro, T. Nishimura, and B. I. Setiawan. 2020. Assessing saturated hydraulic conductivity from the dielectrically-predicted dry bulk density. Agricultural Engineering International: CIGR Journal, 22(3): 43-50.

1 Introduction

Saturated hydraulic conductivity (K_s) is of the main importance of the dynamic status of water in soil (Hillel, 1998). The value of K_s can be used to characterize soil surface runoff, drainage, solute transports, percolation, and runoff (Nishimura et al., 1993; Arya et al., 1998; Malone et al., 2003; Wijaya et al., 2010). Those are determinant for the effectiveness of water and nutrient uptake by plant roots on which the plant growth and yield depend (Kirkham, 2005).

Unfortunately, the measurement of K_s is often found laborious, time consuming, and expensive (Libardi et al., 1980). To deal with this problem, pedotransfer functions for predicting K_s have been extensively expanded by employing the more easily measured soil physical properties: water content (Libardi et al., 1980), effective porosity (Ahuja et al., 1989), moisture retention (Messing,

Received date: 2019-06-10 **Accepted date:** 2019-11-02
***Corresponding author: Krissandi Wijaya,** Faculty of Agriculture, Jenderal Soedirman University, Jl. Dr. Soeparno No. 61, Karangwangkal, Purwokerto 53123, Central Java, Indonesia. Tel: +62-281-638791. Email: krissandi.wijaya@unsoed.ac.id.

1989), air permeability (Loll et al., 1999), and texture (Julia et al., 2004).

In particular, Kozeny-Carman equation (Kozeny, 1927; Carman, 1937) has been able to describe the dry bulk density (ρ_b) dependencies of K_s, and using the similar media concept (SMC) of Miller and Miller (1956), this dependency has been further clarified by Campbell (1985). Miyazaki (1996), on the other hand, has proposed a non-similar media concept (NSMC) for exploring the ρ_b dependencies of K_s, and the result was better than these two preceding models. This NSMC model is applicable to the wide range of soil structure: dispersed to aggregated soils (Miyazaki, 1996), helpful for scaling usage (Zhuang et al., 2000), and yet reliable for compact subsoil (Nakano and Miyazaki, 2005).

About the soil ρ_b, it is one of the most frequently used parameters for describing the physical properties of soil. The direct measurement, however, is yet laborious and time consuming likewise, and thus, is unfavorable for vast area. Wijaya et al. (2003) have proposed the use of dielectrically-predicted dry bulk density ($\rho_{b\text{-}ADR}$) instead. The $\rho_{b\text{-}ADR}$ was assessed from the value of dielectrically-predicted volumetric water content (θ_{ADR}) using an amplitude domain reflectometry (ADR) probe. The model has been found to be applicable for the either of upland and wetland soils (Wijaya et al., 2004; Wijaya and Kuncoro, 2008).

Despite the effectiveness and practical merit of $\rho_{b\text{-}ADR}$ prediction, the $\rho_{b\text{-}ADR}$ dependencies of K_s has yet been paid less attention. Thus, a model for predicting K_s using $\rho_{b\text{-}ADR}$ has been proposed in this study after a slight modification on the previously available NSMC model.

2 Materials and methods

2.1 Land preparation

A plot 7.5 m × 7.5 m of Andisol (Table 1) located at the Experimental Field of Jenderal Soedirman University – Indonesia (7°14'53"S, 109°56'24"E) was selected as a research site. The plot was imaginary divided into 25 rectangles 1.5 m × 1.5 m of which each corner was taken as the point of field measurement and soil sampling (Figure 1). Thus, there were 36 points in total available. Such plot design was performed within a purpose to endorse the study about spatial variability of the data of interest, which will be presented in another paper. The field, in particular, has been followed for years, but annually plowed and harrowed twice for maintenance.

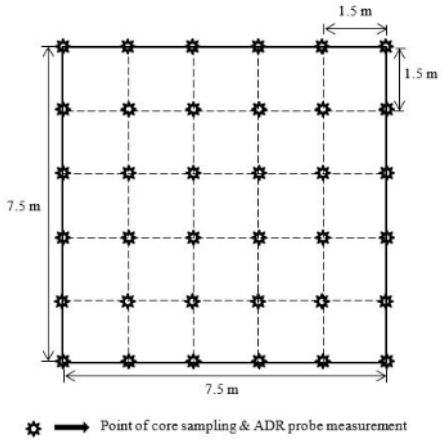

Figure 1 Field schematic diagram of the sampling and measurement points

Table 1 Physical properties of the soil

Parameter (unit)	Value
Texture (%): *Loam*	
Sand	37.4
Silt	48.2
Clay	14.4
Organic carbon content, C-org (%)	9.4
Particle density, ρ_s (g cm^{-3})	2.47
Dry bulk density, ρ_b (g cm^{-3})	0.650
Total density, ρ_t (g cm^{-3})	0.964
Water content at field capacity, *FC* (cm^3 cm^{-3})	0.81
Water content at permanent wilting point, *PWP* (cm^3 cm^{-3})	0.21

2.2 Calibration of ADR probe used

A set of ADR probes that latterly used for field measurement was preliminary calibrated using disturbed samples taken from 0-15 and 15-30 cm soil depths of the targeted field. The samples were mixed and repacked into three acrylic cylinders (11 cm in diameter and 8 cm height) for three levels of soil mass wetness, w (0.30 – 0.80 g g^{-1}) and five levels of total density, ρ_t (0.70 – 1.20 g cm^{-3}). Determination of soil dielectric constant (ν) was performed

by perpendicularly embedding sensor rods of the ADR probe into the targeted sample repacked (Figure 2). This measurement took about 15 seconds for a stable data reading, and has been conducted for three replications of each acrylic cylinder.

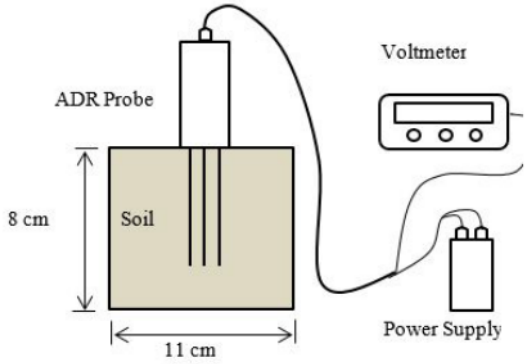

Figure 2 Schematic diagram of the ADR probe calibration

A slight amount of samples, namely about 20 g of each, were taken out of the one third-upper, middle, and lower parts of the acrylic cylinder. These samples were weighed to determine ρ_t, and then oven-dried at 105°C for 24 hours to determine w, by which the value of ρ_b could be calculated from. The data of w and ρ_b were then used to determine the value of volumetric water content (θ) related. Finally, the data of θ and v were plotted and fitted using least-square method (Figure 3) to obtain the model for predicting θ namely θ_{ADR} from the data of v observed:

$$\theta_{ADR} = 2.5582v^3 - 4.7527v^2 + 3.2659v - 0.3970 \quad (1)$$

Where: θ_{ADR} is dielectrically predicted θ (cm^3 cm^{-3}), and v is dielectric constant data (volt).

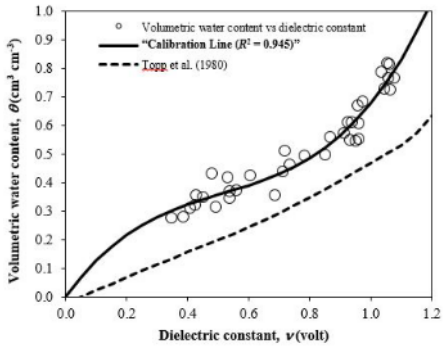

Figure 3 Relationship between volumetric water content, θ (cm^3 cm^{-3}) and dielectric constant, v (volt) after the calibration of ADR probe conducted

2.3 Soil sampling and measurement

The calibrated ADR probe was applied to the targeted measurement point (Figure 1) for data collection of the soil dielectric constant. This measurement was conducted at 0-15 and 15-30 cm soil depths for three replications. Thus, total number of the data collected was 216 of which 108 data were obtained from the each depth. By recalling Equation 1, the data were then employed to determine the related θ_{ADR} as in Wijaya et al. (2003, 2004).

After the measurement, undisturbed soil sample was taken using 100 cm^3 core sampler (5 cm in diameter and 5 cm height) for the same number of replicates and a range of soil depth nearby. The sample was weighed to determine ρ_t and then water saturated for K_s measurement using the falling head method. Finally, the sample was oven-dried at 105°C for 24 hours to determine the value of w and ρ_b, by which the value of θ related could be calculated from.

2.4 Model development

Previously available NSMC model for predicting K_s (Miyazaki, 1996) may be written as:

$$K_s = K_{s0}\left[\frac{\left(\frac{\tau\rho_s}{\rho_b}\right)^{\frac{1}{3}}-1}{\left(\frac{\tau\rho_s}{\rho_{b0}}\right)^{\frac{1}{3}}-1}\right]^2 \quad (2)$$

Where: K_s is predicted saturated hydraulic conductivity (cm s^{-1}), K_{s0} is saturated hydraulic conductivity of the sample reference (cm s^{-1}), τ is shape factor of the solid phase ($\rho_b/\rho_s < \tau \leq 1$), ρ_s is particle density of the sample reference (g cm^{-3}), ρ_b is dry bulk density of the soil sample examined (g cm^{-3}), and ρ_{b0} is dry bulk density of the sample reference (g cm^{-3}).

Meanwhile, the value of $\rho_{b\text{-}ADR}$ could be determined from ρ_t and θ_{ADR} (Wijaya et al., 2003, 2004):

$$\rho_{b-ADR} = \rho_t - (\theta_{ADR}\,\rho_w) \quad (3)$$

Where, $\rho_{b\text{-}ADR}$ is dielectrically-predicted dry bulk density (g cm^{-3}), ρ_t is the total density (g cm^{-3}), θ_{ADR} is

dielectrically-predicted volumetric water content (cm^3 cm^{-3}), and ρ_w is the water density (1 g cm^{-3}).

By substituting ρ_b in the Equation 2 with $\rho_{b\text{-}ADR}$ in Equation 3, a new model for predicting K_s may take shape as:

$$K_{s-ADR} = K_{s0}\left[\frac{\left(\frac{\tau\rho_s}{\rho_{b-ADR}}\right)^{\frac{1}{3}}-1}{\left(\frac{\tau\rho_s}{\rho_{b0}}\right)^{\frac{1}{3}}-1}\right]^2 \quad (4)$$

Where: $K_{s\text{-}ADR}$ is dielectrically-predicted saturated hydraulic conductivity (cm s^{-1}). For the sake of simplicity, we suggested to call this new proposed model as "Dielectric NSMC" in order to distinguish it from the previously available NSMC model.

2.5 Model validation

All those dielectrically-predicted parameters θ_{ADR}, $\rho_{b\text{-}ADR}$, and $K_{s\text{-}ADR}$ were validated using the measured θ, ρ_b, and K_s, respectively. The analysis was performed upon the value of mean difference (MD), root mean square error (RMSE), relative root mean square error (rRMSE), and deviation times (DT):

$$MD = \frac{1}{n}\sum_{i=1}^{n}(PV_i - MV_i) \quad (5)$$

$$RMSE = \sqrt{\frac{1}{n}\sum_{i=1}^{n}(PV_i - MV_i)^2} \quad (6)$$

$$rRMSE = RMSE\frac{100}{MV} \quad (7)$$

$$\log_{10} DT = \sqrt{\frac{1}{n}\sum_{i=1}^{n}\left[\log_{10}\left(\frac{K_{s-ADR}}{K_s}\right)\right]^2} \quad (8)$$

Where: PV is the value of dielectrically predicted parameters (cm^3 cm^{-3}, g cm^{-3}, or cm s^{-1}), MV is the value of measured parameters (cm^3 cm^{-3}, g cm^{-3}, or cm s^{-1}), MV is the mean of measured parameters (cm^3 cm^{-3}, g cm^{-3}, or cm s^{-1}), and n is the sample number.

3 Results and discussion

3.1 Dielectrically-predicted volumetric water content (θ_{ADR})

As shown in Figure 4, there was a tendency for the θ_{ADR} predicted to slightly overestimate the $\theta_{\_meas}$ measured. This result was also implied from the positive value of mean difference (MD) as 0.033 and 0.053 for the both soil depths observed 0-15 and 15-30 cm, respectively (Table 2). The small values of RMSE and rRMSE for these depths, however, suggested a small deviation of the θ_{ADR} from the $\theta_{\_meas}$, and this was also revealed from the scattering pattern of the data with regard to the 1:1 line in Figure 4. These results, in general, suggested that there was a fairly good agreement between the θ_{ADR} and $\theta_{\_meas}$, in line with the result of Wijaya et al. (2003, 2004, 2010).

If we took a look closer to the soil depths, in particular, 15-30 cm depth resulted a slightly higher value of RMSE and rRMSE, rather than the 0-15 cm depth (Figure 4), which implied a bit more discrepancy between the θ_{ADR} and $\theta_{\_meas}$ at this former depth. This result was ascribed to the remaining earthworm furrows or dense layer of this untilled 15-30 cm depth, which may in turn affect the volume of soil macro-pores of the soil pores (McColl et al., 1982; Hillel, 1998; Malone et al., 2003; Domingues et al., 2018; Wijaya et al., 2019), and thus, alter the soil θ as well (Horn et al., 2014; Iiyama and Hirai, 2014). As the θ_{ADR} tended to slightly overestimate $\theta_{\_meas}$, it was due to the remaining dense layer to be more dominant than the remaining earthworm furrows, of which the less volume of macro-pores resulted the less value of $\theta_{\_meas}$.

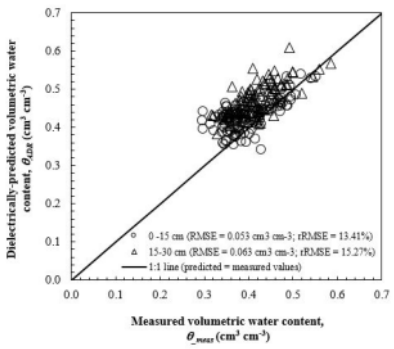

Figure 4 Dielectrically-predicted (θ_{ADR}) vs. measured ($\theta_{\_meas}$) volumetric water content

Table 2 Statistical values for the degree of coincidence between dielectrically-predicted and measured data

Parameter (unit)	Soil depth (cm)	Sample number (n)	MD	RMSE	rRMSE (%)	DT (times)
θ (cm^3 cm^{-3})	0 – 15	108	0.033	0.053	13.41	NA
	15 – 30	108	0.053	0.063	15.27	NA
ρ_b (g cm^{-3})	0 – 15	108	-0.033	0.053	8.90	NA
	15 – 30	108	-0.053	0.064	10.27	NA
K_s (cm s^{-1})	0 – 15	108	-0.00157	0.011	38.11	1.50
	15 – 30	108	-0.00035	0.009	52.84	1.73

3.2 Dielectrically-predicted dry bulk density (ρ_{b_ADR})

There was a tendency for the predicted ρ_{b_ADR} to slightly underestimate the measured ρ_{b_meas} (Figure 5), and this was in line with the negative value of MD as -0.033 and -0.053 for the depth of 0-15 and 15-30 cm, respectively (Table 2). This result, however, was conversely to the case of θ_{ADR} to $\theta_{\_meas}$ shown in Figure 4. In fact, the soil dry bulk density (ρ_b) has a negative correlation with the total soil porosity (e.g. Etana et al., 2013; Kuncoro et al., 2014; Domingues et al., 2018), and thus, with the soil volumetric water content (θ) as well.

Except for the value of ρ_{b_meas} less than 0.47 g cm^{-3}, the scattering pattern of the data with regard to the 1:1 line in Figure 5 implies a relatively small deviation of the ρ_{b_ADR} from the ρ_{b_meas}, which was further explained by the small value of RMSE and rRMSE for the both depths observed. This result, in general, implied that there was a fairly good agreement between the ρ_{b_ADR} and ρ_{b_meas}, and this was in a good agreement with the finding of Wijaya et al. (2003, 2004, 2010).

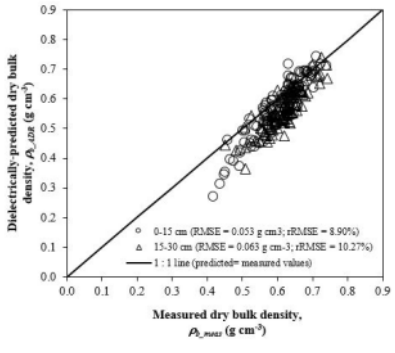

Figure 5 Dielectrically-predicted (ρ_{b_ADR}) vs. measured (ρ_{b_meas}) dry bulk density

In particular, a slightly higher value of RMSE and rRMSE for the depth of 15-30 cm than the depth of 0-15 cm (Figure 5) implied a bit more discrepancy between ρ_{b_ADR} and ρ_{b_meas} for the former depth. Likewise, this result was thought to be ascribed to the remaining earthworm furrows or the development of dense layers of this untilled 15-30 cm depth (McColl et al., 1982; Hillel, 1998; Malone et al., 2003; Kuncoro et al., 2014; Domingues et al., 2018; Wijaya et al., 2019). As the ρ_{b_ADR} tended to slightly underestimate ρ_{b_meas}, more dominant remaining dense layer than the earthworm furrows was the reason for the higher value of ρ_{b_meas}.

3.3 Dielectrically-predicted saturated hydraulic conductivity (K_{s_ADR}) from the "Dielectric NSMC" model developed

The developed "Dielectric NSMC", followed by the NSMC model from Miyazaki (1996), could describe K_{s_ADR} with regard to the ρ_{b_ADR} better than the two other models Kozeny-Carman (Carman, 1937; Campbell, 1985) for the both ranges of soil depth observed (Figure 6). This result was thought to be ascribed to the fitting parameter, namely a shape factor of solid phase (τ) (Table 3) considered in the both "Dielectric NSMC" and NSMC models after Miyazaki (1996).

Further comparing between the "Dielectric NSMC" and NSMC models, the former could characterize ρ_{b_ADR} dependencies of K_{s_ADR} better than the latter (Figure 6) regardless of their same value in τ (Table 3). This difference was more related to the two other fitting parameters K_{s0} and ρ_{b0}. The value of K_{s0} in this study was found to be higher than that of Miyazaki (1996), but this was conversely for the case of ρ_{b0} (Table 3). This result

suggests that special care should be given when specifying K_{s0} and ρ_{b0} since these values might be site specific and soil type dependent.

Adding to this, the number of ρ_b data of interest used for determining those fitting parameters might also be a point of concern: 108 data of predicted $\rho_{b\text{-}ADR}$ in this study, but 18 measured ρ_b of repacked disturbed-samples in Miyazaki (1996). It seems that the larger number of ρ_b data used for, the smoother fitting parameters will be resulted. In this manner, therefore, the effectiveness and practical merit of ρ_b prediction using ADR probe proposed in this study provide a certain advantage compared to the conventional direct measurement of ρ_b.

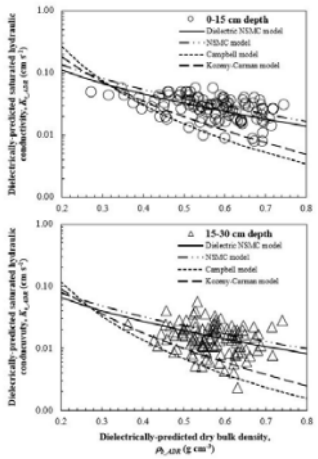

Figure 6 Dielectrically-predicted saturated hydraulic conductivity (K_{s_ADR}) vs. dielectrically-predicted dry bulk density (ρ_{b_ADR})

Table 3 Fitted parameters for the K_s prediction

Soil depth (cm)	Sample number (n)	Dielectric NSMC model developed			NSMC model (Miyazaki, 1996)		
		K_{s0} (cm s^{-1})	ρ_{b0} (g cm^{-3})	τ	K_{s0} (cm s^{-1})	ρ_{b0} (g cm^{-3})	τ
0 – 15	108	0.0653	0.306	0.96	0.0535	0.404	0.96
15 – 30	108	0.0412	0.294	0.96	0.0383	0.354	0.96

Considering about the soil depths, on the other hand, K_{s_ADR} of 15-30 cm depth was found a bit more scattered than that of 0-15 cm depth, especially for the higher ρ_{b_ADR} namely more than 0.62 g cm^{-3} (Figure 6). This result was in line with the aforementioned higher discrepancy of the θ_{ADR} and ρ_{b_ADR} for this depth of interest (Figure 4 and Figure 5, respectively). This was related to the variety in soil macro-pores volume due to the remaining earthworm furrows or dense layer of this untilled 15-30 cm depth (McColl et al., 1982; Hillel, 1998; Ahuja et al., 1989; Arya et al., 1998; Horn et al., 2014; Domingues et al., 2018; Wijaya et al., 2019).

3.4 Dielectrically-predicted (K_{s_ADR}) vs. measured (K_{s_meas}) saturated hydraulic conductivity

There was a tendency for the K_{s_ADR} to slightly underestimate K_{s_meas} (Figure 7), similar to the case of the aforementioned ρ_{b_ADR} to ρ_{b_meas} (Figure 5). This result was further supported by the negative value of MD as -0.00157 and -0.00035 for the both depths observed 0-15 and 15-30 cm, respectively (Table 2). Nevertheless, the small values of RMSE and rRMSE for these depths (Table 2) indicated a small deviation of the K_{s_ADR} from the K_{s_meas}. This was in accordance with the scattering pattern of the data with regard to the 1:1 line in Figure 7 except for the K_{s_meas} data less than 0.004 cm s^{-1} of 15-30 cm depth. This result, in general, suggested that there was a fairly good agreement between the K_{s_ADR} and K_{s_meas}. Thus, the developed "Dielectric NSMC" model was considerably sufficient for predicting K_s upon the Andisol soil observed in this study.

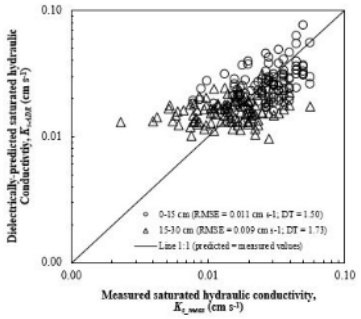

Figure 7 Dielectrically-predicted (K_{s_ADR}) vs. measured (K_{s_meas}) saturated hydraulic conductivity.

Comparing between the two 0-15 and 15-30 cm depths observed, the latter tended to result more scattered data of K_{s_ADR} with regard to K_{s_meas} than the former, regardless of

the lower RMSE value of the latter (Figure 7). This discrepancy might be explained by the higher values of rRMSE and DT of the latter than that of the former (Table 2). In addition, the latter tended to result lower K_{s_ADR} than the former for a certain ρ_{b_ADR} given as shown in Figure 6. This result, however, was different from the finding of Nakano and Miyazaki (2005) that K_s of untilled subsoil was well related with its ρ_b by the NSMC model and always higher than the K_s of tilled topsoil.

The difference was probably related to the type of soil observed: Eutric Fluvisol in Nakano and Miyazaki (2005), but Andisol in this study. Further, site specific characteristics of the soil structure might also be a point of concern. Nakano and Miyazaki (2005) have assumed that untilled subsoil tends to be compacted without serious changes in micromorphology of soil pores, while we thought about changes in the volume of macro-pores due to the remaining earthworm furrows or dense layer of this untilled 15-30 cm depth (McColl et al., 1982; Hillel, 1998; Malone et al., 2003; Wijaya et al., 2010; Etana et al., 2013; Domingues et al., 2018; Wijaya et al., 2019).

4 Conclusion

Predicted dry bulk density ($\rho_{b\text{-}ADR}$) using ADR probe has been employed to predict saturated hydraulic conductivity (K_{s_ADR}) after a slight modification on the previously available NSMC model. The proposed "Dielectric NSMC" model could describe ρ_{b_ADR} dependencies of K_{s_ADR} better than the other proceeding models for both ranges 0-15 and 15-30 cm of soil depths observed. This proposed model tended to slightly underestimate the measured saturated hydraulic conductivity (K_{s_meas}) as implied from the negative value of MD. The scattering pattern of data which was well supported by the small value of RMSE and rRMSE, however, suggested a small deviation of the K_{s_ADR} from the K_{s_meas}. In general, therefore, the proposed model was considerably sufficient for characterizing ρ_{b_ADR} dependencies of K_{s_ADR}.

Acknowledgement

This study was partly supported by the Directorate General for Higher Education of The Ministry of Research, Technology, and Higher Education of Indonesia. The authors are grateful to Dr. Tetsuya Araki for the very valuable discussion and constructive suggestion. Further, the authors acknowledged Dr. Ardiansyah for the inspiring idea during the data collection.

References

Ahuja, L. R., D. K. Cassel, R. R. Bruce, and B. B. Barnes. 1989. Evaluation of spatial distribution of hydraulic conductivity using effective porosity data. *Soil Science*, 148(6): 404-411.

Arya, L. M., T. S. Dierolf, A. Sofyan, I. Widjaja-Adhi, and M. T. Van-Genuchten. 1998. Field measurement of the saturated hydraulic conductivity of a macroporous soil with unstable subsoil structure. *Soil Science*, 163(11): 841-852.

Campbell, G. S. 1985. *Soil Physics with Basic: Transport Model for Soil-Plant Systems*. Amsterdam: Elsevier.

Carman, P. C. 1937. Fluid flow through granular beds. *Transaction of the Institution of Chemical Engineers*, 15: 150-166.

Domingues, R., A. B. Pereira, L. F. Pires, L. M. Schiebelbein, E. A. Barbosa,and A. C. Auler. 2018. Beans cultivation and water regime on soil physical attributes. *Agricultural Engineering International: CIGR Journal*, 20(3): 13–23.

Etana, A., M. Larsbo, T. Keller, J. Arvidsson, P. Schjønning, J. Forkman, and N. Jarvis. 2013. Persistent subsoil compaction and its effects on preferential flow patterns in a loamy till soil. *Geoderma*, 192: 430-436.

Hillel, D. 1998. *Environmental Soil Physics*. San Diego: Academic Press.

Horn, R., X. Peng, H. Fleige, and J. Dörner. 2014. Pore rigidity in structured soils—only a theoretical boundary condition for hydraulic properties? *Soil Science and Plant Nutrition*, 60(1): 3–14.

Iiyama, I., and T. Hirai. 2014. Subsoil water available in suction and poor in amount under continuous grassland use. *Soil Science and Plant Nutrition*, 60(4): 439–447.

Julia, M. F., T. E. Monreal, A. S. C. Jimenez, and E. G. Melendez. 2004. Constructing a saturated hydraulic conductivity map of spain using pedotransfer function and spatial prediction. *Geoderma*, 123: 257-277.

Kirkham, M. B. 2005. *Principles of Soil and Plant Water Relations*. Boston: Elsevier Academic Press.

Kozeny, J. 1927. *Soil Permeability*. Sitzungsber Akad. Wiss, Wien, 136(2a): 271.

Kuncoro, P. H., K. Koga, N. Satta, and Y. Muto. 2014. A study on the effect of compaction on transport properties of soil gas and water I: Relative gas diffusivity, air permeability, and saturated hydraulic conductivity. *Soil and Tillage Research*, 143: 172-179.

Libardi, P. L., K. Reichardt, D. R. Nielsen, and J. W. Biggar. 1980. Simple field method for estimating soil hydraulic conductivity. *Soil Science Society of America Journal*, 44(1): 3-7.

Loll, P., P. Moldrup, P. Schjønning, and H. Riley. 1999. Predicting saturated hydraulic conductivity from air permeability: Application in stochastic water infiltration modeling. *Water Resources Research*, 35(8): 2387-2400.

Malone, R. W., S. Logson, M. J. Shipitalo, J. Weatherington-Rice, L. Ahuja, and L. Ma. 2003. Tillage effect on macroporosity and herbicide transport in percolate. *Geoderma*, 116(1-2): 191-215.

McColl, H. P., P. B. S. Hart, and F. J. Cook. 1982. Influence of earthworms on some soil chemical and physical properties, and the growth of ryegrass on a soil after topsoil strippingÜa pot experiment. *New Zealand Journal of Agricultural Research*, 25(2): 239-243.

Messing, I. 1989. Estimation of the saturated hydraulic conductivity in clay soils from soil moisture retention data. *Soil Science Society of America Journal*, 53(3): 665-668.

Miller, E. E., and R. D. Miller. 1956. Physical theory for capillary flow phenomena. *Journal of Applied Physics*, 27(4): 324-332.

Miyazaki, T. 1996. Bulk density dependence of air entry suctions and saturated hydraulic conductivities of soils. *Soil Science*, 161(8): 484-490.

Nakano, K., and T. Miyazaki. 2005. Predicting the saturated hydraulic conductivity of compacted subsoils using the non-similar media concept. *Soil and Tillage Research*, 84(2): 145-153.

Nishimura, T., M. Nakano, and T. Miyazaki. 1993. Properties of surface crusts of an Andisol and their effects on soil hydrological processes. *Catena Supplements*, 24: 17-28.

Wijaya, K., and P. H. Kuncoro. 2008. Application of dielectric constant method to predict spatial variability of soil permeability on potato field. *Jurnal Inovasi*, 1(2): 67-77 (in Indonesian with abstarct in English).

Wijaya, K., T. Nishimura, and M. Kato. 2003. Estimation of dry bulk density of soil using amplitude domain reflectometry probe. *Journal of the Japanese Society of Soil Physics*, 95: 63-73.

Wijaya, K., T. Nishimura, M. Kato, and M. Nakagawa. 2004. Field estimation of soil dry bulk density using amplitude domain reflectometry data. *Journal of the Japanese Society Soil Physics*, 97: 3-12.

Wijaya, K., T. Nishimura, B. I. Setiawan, and S. K. Saptomo. 2010. Spatial variability of soil hydraulic conductivity in paddy field in accordance to subsurface percolation. *Paddy and Water Environment*, 8(2): 113-120.

Wijaya, K., P. H. Kuncoro, and P. Arsil. 2019. Dynamics of soil physical and chemical properties within horizontal ridges-organic fertilizer applied potato land. *IOP Confernece Series: Earth Environmental Science*, 255: 012024.

Zhuang, J., K. Nakayama, G. R. Yu, and T. Miyazaki. 2000. Scaling of saturated hydraulic conductivity: a comparison of models. *Soil Science*, 165(9): 718-727.

Krisandi-(3)_Assessing saturated hydraulic conductivity from the dielectrically-predicted dry bulk density

ORIGINALITY REPORT

10%	10%	9%	3%
SIMILARITY INDEX	INTERNET SOURCES	PUBLICATIONS	STUDENT PAPERS

MATCHED SOURCE

1	link.springer.com Internet Source	2%

2%

★ link.springer.com

Internet Source

Exclude quotes	On	Exclude matches	< 1%
Exclude bibliography	On		